The IP-10 Chemokine Binds to a Specific Cell Surface Heparan Sulfate Site Shared with Platelet Factor 4 and Inhibits Endothelial Cell Proliferation

By Andrew D. Luster,* Sheryl M. Greenberg,‡ and Philip Leder*

From the *Department of Genetics, Harvard Medical School, Howard Hughes Medical Institute, Boston, Massachusetts 02115; and ‡Repligen Corporation, Cambridge, Massachusetts 02139

Summary

IP-10 is a member of the chemokine family of cytokines and is induced in a variety of cells in response to interferon γ and lipopolysaccharide. The self-aggregation common to many chemokines, including IP-10, has hindered the identification of a specific IP-10 receptor. Using an IP-10 alkaline phosphatase fusion protein that fortuitously blocks this self-aggregation, we have identified an IP-10 binding site on a variety of cells including endothelial, epithelial, and hematopoietic cells. This binding site has a K_d of 25 nM, is inhibited by recombinant murine or human IP-10, and is dependent on the presence of cell surface heparan sulfate proteoglycans (HSPG). This conclusion is based on the findings that IP-10 binding to cells is: (a) inhibited by heparin and heparan sulfate; (b) sensitive to a 1 M NaCl wash; (c) eliminated by treatment with heparinase and trypsin; and (d) absent on mutant CHO cells that do not express cell surface HSPG. Platelet factor 4 (PF4), but not IL-8, monocyte chemoattractant protein-1, RANTES, monocyte inflammatory protein (MIP)-1α, or MIP-1β, can compete effectively with IP-10 for binding to the cell surface. Furthermore, IP-10 shares with PF4 the ability to inhibit endothelial cell proliferation (IC$_{50}$ = 150 nM). These studies demonstrate specificity in the interaction of chemokines and HSPG, and they define IP-10 and PF4 as a distinct subset of chemokines sharing an HSPG-binding site and angiostatic properties.

IP-10 was identified as an abundant RNA induced by IFN-γ and lipopolysaccharide (2, 3) and encodes a 10-kD secreted protein. It is a member of the -C-X-C- (or α) chemokine family of secreted 8–10-kD proteins and is 31% identical to platelet factor 4 (PF4)[1] and 26% identical to IL-8, two other members of the -C-X-C- chemokine family. IP-10 expression is induced in a variety of tissues in inflammatory conditions, such as psoriasis (4), fixed drug eruptions (5), cutaneous delayed-type hypersensitivity reactions (6), experimental glomerulonephritis (7), and in experimental allergic encephalomyelitis (8). IP-10 also has a potent in vivo antitumor effect that is T cell dependent (9). IP-10 may be a chemoattractant for T cells and monocytes, and it may induce T cells to adhere to activated endothelial cells (10), although these latter in vitro findings remain controversial (11).

Chemokine receptors are known to be promiscuous, binding more than one chemokine, and various leukocytes are known to have more than one chemokine receptor, making interpretation of binding data difficult. The recent molecular cloning of several chemokine receptors, including monocyte inflammatory protein (MIP)-1α/RANTES, monocyte chemoattractant protein (MCP)-1, and the erythrocyte chemokine receptors, as well as the demonstration of binding and signaling in heterologous cells, has been important in clarifying receptor-ligand interactions (12). All the chemokine receptors cloned to date are members of the G protein–coupled seven transmembrane spanner family, and, with the exception of the promiscuous erythrocyte chemokine receptor (which is the Duffy blood group antigen), they induce transient rises in intracellular calcium upon activation. To date, however, a signaling receptor has not been identified for several chemokines, including IP-10 and the first chemokine to be identified, PF4. PF4 has been shown to bind to cell surface heparan sulfate proteoglycans (HSPG) (13, 14) and may, in fact, exert its biological effects of tumor inhibition and angiostasis by displacing growth factors such as basic fibroblast growth factor (bFGF) (15) and TGF-β (16), which use cell surface HSPG as part of their receptor complexes.

To identify IP-10's cellular targets and to help clarify its physiological function and mechanism of signal transduction, we have set out to identify and characterize its specific cell

---

surface receptor. In our initial studies, we found that IP-10, like many other chemokines, aggregates in solution and on the plasma membrane, hampering attempts at obtaining equilibrium-binding constants using radiolabeled IP-10. To overcome this problem, we have constructed an IP-10–alkaline phosphatase (IP-10-AP) fusion gene that, when introduced into mammalian cells, results in the secretion of a nonaggregating monomeric fusion protein that can bind to cells via its NH2-terminal IP-10 epitope and then be enzymatically assayed via its COOH-terminal alkaline phosphatase tail. Using this fusion protein, we have found a specific, non–calcium fluxing, cell surface heparan sulfate (HS) binding site for IP-10 on a variety of cells. This binding site is shared with PF4, and we now find that IP-10 also shares with PF4 the ability to inhibit endothelial cell proliferation.

Materials and Methods

Materials. Heparin was obtained from Hepar Inc. (Franklin, OH). Heparan sulfate, chondroitin sulfate A, chondroitin sulfate B, heparinase I, and heparinase III (heparitinase I) were obtained from Sigma Immunochemicals (St. Louis, MO; catologue Nos. H-7641, C-0914, C-2431, H-2519 and H-889, respectively). Human rIL-8 was purchased from Genzyme Corp. (Cambridge, MA); human rMIP-1α, MIP-1β, RANTES, and MCP-1 were initially supplied by Dr. Tom Schall (Genentech, South San Francisco, CA) and then subsequently purchased from PeproTech, Inc. (Rocky Hill, NJ). Human rPF4 was supplied by Repligen (Cambridge, MA).

Cell Lines and Cell Culture. Cell lines were obtained from American Type Culture Collection (Rockville, MD) with the following exceptions: the SV-40–transformed murine endothelial cell line SVEC (17) was obtained from Dr. Kathryn A. O'Connell (Johns Hopkins University, Baltimore, MD) and CHO K1, 803, and 677 were obtained from Dr. J. Esko (University of Alabama, Birmingham, AL). The 803 and 677 cell lines are mutant CHO cells, defective in HS synthesis, derived from CHO-K1 parental wild-type CHO cells (18). Mutant 803 produces 5–10% residual HS and about one-half the normal level of chondroitin sulfate. Mutant 677 does not synthesize HS and overexpresses chondroitin sulfate by a factor of 3 so that the total amount of sulfated glycosaminoglycan is comparable in 677 and wild-type cells. Mutant 677 lacks both N-acetylglucosaminyltransferase and glucuronosyltransferase, enzymes required for the polymerization of HS chains (19). Human peripheral blood leukocytes and leukocytes nonadherent to nylon wool were kindly provided by Dr. Robert Finberg (Dana Farber Cancer Institute, Boston, MA). Leukocytes were grown in RPMI supplemented with 10% fetal bovine serum (FBS) (Sigma), fibroblast lines and SVEC cells were grown in DMEM (Sigma) supplemented with 10% enriched calf serum (Sigma), human umbilical cord vein endothelial cells (HUVECs) (Clonetics, San Diego, CA) were grown in M199 (GIBCO BRL, Gaithersburg, MD) supplemented with 10% heat-inactivated FBS and 5 ng/ml bFGF (R & D Systems, Inc., Minneapolis, MN), and wild-type and mutant CHO cells were grown in Ham's F12 medium (GIBCO BRL) supplemented with 10% FBS. All media were supplemented with 50 U/ml penicillin, 50 μg/ml streptomycin, and 2 mM L-glutamine; in addition, the murine leukocyte lines were supplemented with 57 μM 2-ME. All cells were maintained at 37°C and 5% CO_2. Bone marrow cells were harvested from the femurs of pathogen-free FVB female mice as described (20) and were maintained either

in 30% L cell–conditioned medium (source of macrophage colony-stimulating factor) and 20% FBS for 2 wk to obtain macrophages or 50% WEHI-conditioned medium (source of IL-3) for 4 wk to obtain mast cells (21).

Protein Expression and Purification. Recombinant murine IP-10 (2) beginning with the putative mature NH2-terminal Ile (nucleotide 129) and terminating with the COOH-terminal Pro (nucleotide 359) and human rIP-10 (1) beginning with the mature NH2-terminal Val (nucleotide 132) and terminating with the COOH-terminal Pro (nucleotide 363) were engineered by PCR using the murine IP-10 (9) and human IP-10 (1) cDNAs as templates, respectively, into the Bam H1 site of the Qiaexpress vectors pQE12 and pQE8 (QIAGEN Inc., Chatsworth, CA) and then transformed into the *Escherichia coli* strain M15. Expression of IP-10 in pQE12 results in a fusion protein containing a (His)6 carboxy-terminal tag and expression of IP-10 in pQE8 results in a fusion protein containing an amino-terminal six histidine tag. In addition, both vectors also result in the addition of Met-Arg-Gly-Ser at the amino terminus of the His-tagged proteins. rIP-10 was purified by sedimentation of inclusion bodies through sucrose, solubilization of the inclusion bodies in 4 M guanidine HCl, affinity chromatography on nickel agarose (QIAGEN Inc.), and reverse phase HPLC (Waters Chromatography, Milford, MA). HPLC was performed on a C18 Vydac (Hespirio, CA) column (2.2 cm I.D.) at a flow rate of 9.5 ml/min, monitoring absorbance at 214 and 277 nm. The column was eluted with a linear gradient of increasing acetonitrile concentration. The specific conditions were: 5% B for 5 min, 5–50% B over 30 min, 50–90% B over 15 min, and then 95% B for 15 min with B being 80% acetonitrile/0.054% TFA acid and the remaining percentage being A, which was 0.06% TFA in water. For the studies reported in this paper, after HPLC purification and lyophilization, IP-10 was dissolved in PBS; however, it was subsequently found that IP-10 was more soluble and aggregated less when it was dissolved in water. The concentration of purified protein was determined with a Bradford assay (Bio-Rad Laboratories, Melville, NY) with BSA and bovine γ-globulin as standards.

Two eukaryotic expression systems were used to express human IP-10: a murine Moloney virus long terminal repeat–based vector (9) transfected into J558L plasmacytoma cells and a dihydrofolate reductase (DHFR) resistance plasmid, pJOD-S (22), transfected into the double DHFR deletion mutant CHO line DG44 (23). The complete human IP-10 coding sequence, the 5' Pst1-Cla1 fragment (nucleotides 1–384) of the human IP-10 cDNA, was blunt-end ligated into the EcoRI site of a MoLTR-SV40 I/pA-expression vector that had been treated with the Klenow fragment of DNA polymerase. Transfection of J558L plasmacytoma cells was performed by electroporation (24). 20 μg of linearized MoLTR-IP10 expression vector plasmid DNA and 1 μg of linearized neomycin resistance plasmid pSV7Neo were used to transfect 5 × 10⁶ cells. After 48 h in RPMI medium, cells were centrifuged and resuspended in selective media containing 0.8 mg/ml of G418 (as calculated for 100% antibiotic activity; Geneticin; GIBCO BRL) and plated in serial dilutions into 96 well plates to clone by limiting dilution. G418-resistant cells from single wells were expanded and a second round of cloning by limiting dilution in selective media was performed to ensure clonality. One clone, 4B6, expressing ∼20 ng/ml IP-10, as determined by a solid-phase ELISA (9), was chosen as the source of secreted IP-10. To try to obtain higher levels of IP-10 secretion, a second eukaryotic expression system using a one-step methotrexate selection was used. For this purpose, the complete coding sequence of human IP-10 was engineered into the SalI site of the mammalian expression vector pJOD-S by blunt-end ligation. 200 μg of the expression plasmid pJOD-IP10 linearized with

Aat II and 200 μg of sonicated herring sperm DNA were electroporated into the DHFR-deficient CHO clone DG44 as described (22). A one-step amplification with 0.5 μM methotrexate (Sigma) was performed in 10% dialyzed FBS and MEM-α lacking ribonucleotides and deoxyribonucleotides (GIBCO BRL). Individual clones were picked after 14 d of selection by ring isolation and expanded. 25 clones were initially assayed for the level of IP-10 expression by Northern blot and immunoblot using rabbit anti-IP10 antiserum. Clone 12D3G4 expressed ∼10 ng/ml of IP-10 (as determined subsequently by ELISA) and was chosen as the source of secreted IP-10. Conditioned medium from transfected cells grown in serum free medium (Nutridoma from Boehringer Mannheim for J558L; CHO-S-SFM from GIBCO BRL for CHO cells) was collected and passed over a heparin Sepharose column (Pharmacia Fine Chemicals, Piscataway, NJ). After step elutions with a NaCl gradient, an aliquot of each fraction was analyzed by SDS-PAGE and Western blotting using an affinity-purified rabbit anti–IP-10 antibody (25). The fraction containing IP-10 immunoreactive material was then purified by reverse-phase HPLC using the acetonitrile gradient previously described. HPLC fractions were then analyzed by SDS-PAGE on a 12.5% SDS-polyacrylamide gel using a Tris/Tricine buffer system (26) that has good resolution in the low molecular weight region, followed by either Coomassie staining or Western blotting using rabbit anti–human IP-10 antisera (see below). IP-10 purified from J558L and CHO had the same appearance on SDS-PAGE.

Antibody Preparation. For immunizations, both human and murine IP-10 were purified from *E. coli* as described above, except that the eluate from the nickel-agarose chromatography column was separated on a denaturing SDS-polyacrylamide gel. The region of the gel containing IP-10 was cut out and emulsified with complete Freund's adjuvant for the primary immunization and with incomplete Freund's adjuvant for subsequent immunizations. Three 8-wk-old female New Zealand white rabbits were injected subcutaneously with ∼200 mg per rabbit of the carboxy-terminal tagged protein (IP-10-(His)₆). The rabbits were boosted twice, at 1-mo intervals, with 100 mg of the amino-terminal tagged protein ((His)₆-IP-10) per rabbit to ensure the generation of antibodies recognizing the native NH₂ and COOH termini of IP-10. 10 d after the second boost, the three rabbits were bled, and the serum was isolated and a portion was pooled for affinity purification. Affinity purification of antiserums was performed as described (25) using the His-tagged rIP-10 coupled to CNBr-activated Sepharose beads (Pharmacia).

Radiolabeling rIP-10. IP-10 purified from *E. coli* was labeled with the ¹²⁵I Bolton and Hunter reagent (Amersham) according to the manufacturers instructions and unincorporated ¹²⁵I-Bolton and Hunter reagent was removed on a NAP-5 column (Pharmacia). The Bolton and Hunter reagent was chosen to radiolabel IP-10 because IP-10 contains no tyrosines amenable to chemical modification with ¹²⁵I. Radiolabeled IP-10 (specific activity = 154 ng/μCi) was also supplied by Dr. Garth Brown (NEN/DuPont) who radiolabeled PeproTech IP-10 by the Bolton and Hunter method and then purified it by reverse phase HPLC.

Production of IP-10–AP Fusion Protein. Human and murine IP-10 was expressed as a soluble fusion protein with the secreted form of placental alkaline phosphatase (AP) by engineering the human and mouse cDNAs for IP-10 into the APtag vector (27). This was accomplished by PCR using the 5' primer CGCAAGCTTCGG-GAGACATTCCTCAATTGC and the 3' primer CGCGGATC-CAGGAGATCTTTTAGACATTTC for human IP-10, as well as the 5' primer ACAGATCTAAGCGCTTCATCCACCGCTGA and the 3' primer GCGAGATCTAGGAGCCCTTTTAGACCTTTT for murine IP-10 and the human and mouse IP-10 cDNA clones as

templates, respectively. After digestion of the human PCR product with HindIII and BamHI and the mouse PCR product with BglII, they were ligated into the HindIII/BglII and BglII site of the APtag vector, respectively. This resulted in fusion proteins that contained the authentic signal sequences and entire mature proteins fused in frame with secreted AP (SEAP) via the four–amino acid linker Gly-Ser-Ser-Gly for human IP-10 and Arg-Ser-Ser-Gly for murine IP-10.

The IP-10–APtag plasmids linearized with SalI were co-transfected with the selectable marker pSV7neo into NIH-3T3 cells by the calcium phosphate method. After selection with 0.4 mg/ml G418 (GIBCO BRL) in 96-well plates (6.4 mm per well), ∼100 individual clones were screened for secreted alkaline phosphatase activity. This assay was performed by heating 50 μl of the supernatant at 65°C for 10 min to inactivate background cellular phosphatase activity and then measuring the A₄₀₅ on a V_max kinetic microplate reader (Molecular Devices, Menlo Park, CA) after incubating with 1 M diethanolamine, pH 9.8, 0.5 mM MgCl₂, 10 mM L-homoarginine (a phosphatase inhibitor), and 12 mM p-nitrophenyl phosphate (Sigma), all prepared as a 2× stock solution (SEAP buffer). The highest expressing NIH-3T3 clones, 18.G5 for murine and 17.G2 for human IP-10–AP produced 1,000 mOD/ml per min and 800 mOD/ml per min, respectively, were used for the experiments described in this paper. A control NIH-3T3 clone expressing unfused SEAP was produced by transfecting with plasmid pBC12/CMV/ SEAP. Other control fusion proteins such as, human and murine IL-4–AP and kit-AP were kindly provided by Drs. B. Morrison (Dana Farber Cancer Institute, Boston, MA) and J. Flannagan (Harvard Medical School, Boston, MA), respectively.

To determine the specific activity of the proteins, the concentration of IP-10–AP in the supernatant was estimated by quantitative immunoprecipitation (see below) followed by SDS-PAGE with Coomassie blue staining and comparing the intensity of Coomassie staining compared to BSA standard dilution. To determine the efficiency of immunoprecipitation, the amounts of AP activity in the initial sample and the remaining AP activity next two sequential immunoprecipitations were determined and used as a correction factor to calculate for <100% efficiency of immunoprecipitation. The resulting estimate for the specific activity of murine IP-10–AP was 30 mOD/min per ng, which is similar to the specific activity determined for IL-4–AP (100 mOD/min per ng; reference 38).

Immunoprecipitation and Immunoblotting. 1 ml of conditioned media from the NIH-3T3 clone 18.G5 secreting mIP-10–AP was collected, centrifuged at 1,000 g, and protease inhibitors (Boehringer Mannheim Biochemicals) were added to the supernatant at the following concentrations: leupeptin (0.3 ng/ml), aprotinin (10 ng/ml), PMSF (20 ng/ml), and pepstatin (0.8 ng/ml). The supernatant was then centrifuged at 10,000 g for 30 min at 4°C and then precleared for 4 h at 4°C with 50 μl of a 1:1 slurry of protein A–Sepharose (PAS) (Pharmacia). The PAS was then centrifuged at 10,000 g in eppendorf tubes, and 50 μl of a 1:1 slurry of a mAb to placental AP (catalogue No. A-018-02; Medix Biotech, Foster City, CA) coupled to CNBr-activated Sepharose (Pharmacia) was added to the supernatant for 2 h at 4°C. The beads were recovered by centrifugation at 10,000 g for 10 min and a second immunoprecipitation was performed by adding another 50 μl of a 1:1 slurry of mAb-Sepharose beads and incubating for another 2 h at 4°C. The immunoprecipitates were then washed 3× with 1 ml of RIPA buffer (0.15 M NaCl, 1% NP-40, 0.1% SDS, 0.5% deoxycholate, 0.05 M Tris, pH 8.0) and then boiled for 3 min in 50 μl of sample buffer containing 0.3 M 2-ME, 4% SDS. 20 μl was then analyzed on a Laemmli 10% SDS-polyacrylamide gel and the intensity of Coomassie staining was compared to a dilution series of BSA.

For immunoblotting, gels were transferred to Immobilon-P mem-

branes (Millipore Corp., Bedford, MA) with a semidry transblotter (Owl Scientific, Woburn, MA) blocked with 3% nonfat dry milk/3% goat serum (Sigma)/PBS and incubated with a 1:10,000 dilution of affinity-purified rabbit anti–IP-10 antiserum for 2 h at room temperature. The membranes were then washed 2× 10 min each with PBS/.1% Tween 20, 1× 10 min with RIPA buffer, and then 2× 10 min each with PBS/.1% Tween 20, and then incubated with a 1:20,000 dilution of peroxidase-conjugated goat anti–rabbit IgG (catalogue No. 111-035-003; Jackson ImmunoResearch Laboratories, West Grove, PA) for 1 h at room temperature in 3% nonfat milk and 3% goat serum in PBS. The membrane was then washed as described above and developed using an ECL chemiluminescence kit (Amersham).

Binding Assays. For nonadherent cells, 10^7 cells were washed 1× with ice-cold binding buffer (HBSS/10 mM Hepes/0.1% BSA) and resuspended in the indicated concentration of IP-10–AP and competitors in a total of 100 μl ice-cold binding buffer. Binding was carried out for 2 h on ice with occasional mixing. Cells were washed 5× with ice-cold binding buffer by repeated centrifugation at 4°C. Cell-bound AP activity was determined by lysing cells in 100 μl of 10 mM Tris, pH 8.0/1% Triton X-100, heating at 65°C for 10 min to inactivate cellular AP, and then centrifuging at 14,000 g for 10 min. 50 μl of the soluble lysate was then mixed with 50 μl 2× SEAP buffer in a 96-well plate at room temperature, and the colormetric product was assayed in a kinetic plate reader at A_{405}. For adherent cells with higher numbers of binding sites, binding was determined in six-well cluster plates. Cells were washed 2× with ice-cold binding buffer and incubated with the indicated concentration of IP-10–AP and competitor in a total of 500 μl of ice-cold binding buffer for 2 h in the cold room on a rocker platform. Cells were washed 6× with binding buffer, lysed with 100 μl of 10 mM Tris, pH 8.0/1% Triton X-100, scraped into an Eppendorf tube, and then assayed as described above. Nonspecific binding was determined in one of two ways. For the calculation of the equilibrium constant, nonspecific binding was determined by adding 10 mM rIP-10 at each concentration of IP-10–AP and performing the binding experiments in parallel exactly as described above. Specific binding was determined by subtracting background from total binding. Specific binding data was analyzed with the binding equation $B = (B_{max} \times F)/(K_d + F)$, where B is bound ligand and F is free ligand (28), using the program KaleidaGraph (Synergy Software, Reading, PA) on a Macintosh computer. For other experiments, nonspecific binding was determined by adding equal amounts of nonfusion SEAP or cross-species IL-4–AP (hIL-4 does not bind to mouse cells and mouse IL-4 does not bind to human cells) and performing the binding experiments in parallel exactly as described above. To obtain IP-10– AP at concentrations higher than the concentration found in the conditioned medium of transfected cells, transfected cells were maintained in serum-free DMEM for 14 d and the conditioned medium was concentrated 100-fold by ultrafiltration (Amicon Corp., Beverly, MA). ^{125}I-IP-10 binding to cells was performed essentially as described above for IP-10–AP binding, except the cell pellet with bound IP-10 was counted in a gamma counter.

Heparinase and Trypsin Treatment. For adherent cells, 10^6 cells were washed 1× with serum-free DMEM and then incubated in 500 μl serum-free DMEM at 37°C and 5% CO_2 for 1 h with either 2.5 U/ml heparinase I or 0.2 U/ml heparinase III (heparitinase) (29). For nonadherent cells, 10^7 cells were washed 1× with serum-free RPMI and resuspended in 100 μl RPMI plus the concentrations of Heparinase I and III indicated above. After enzyme treatment, adherent cells were washed 4× with 5 ml binding buffer and nonadherent cells were washed 2× with 10 ml binding buffer, then assayed

for IP-10–AP binding as described above. Confluent monolayers ($\sim$$10^7$ cells) of adherent cells were washed 1× with calcium- and magnesium-free HBSS and incubated for 5 min 37°C and 5% CO_2 with 0.25% trypsin/0.02% EDTA (JRH Biosciences, Lexena, KA). After enzyme treatment, the cells were washed with 10 ml DMEM/10% FBS and 10 ml binding buffer, and then resuspended in 100 μl binding buffer and assayed for IP-10–AP binding as described above.

Endothelial Cell Proliferation Assay. HUVECs were routinely used between passages 17 and 30. Cellular proliferation was determined by incorporation of [^{3}H]thymidine into DNA as previously described (30). Briefly, rhIP-10 and rhPF4 were added to HUVECs plated in 96 well plates (6 × 10^3 cells per well) grown in M199/10% FBS/5 ng/ml FBS. 3 d later, the amount of [^{3}H]thymidine incorporated into DNA per well was determined. Samples were tested in triplicate.

Calcium Flux. THP-1, A20, and EL4 cells were resuspended at 2 × 10^6 cells per ml in RPMI 1640 containing 2% FBS and 5 μg/ml Fura 2-am (Molecular Probes Inc., Eugene, OR) (diluted from a 1 mg/ml stock in dimethyl sulfoxide). THP-1 cells were incubated for 1 h, and A20 and EL4 cells were incubated for 30 min at 37°C and were then washed three times in 145 mM NaCl, 4 mM KCl, 1 mM NaH_2PO_4, 0.8 mM $MgCl_2$, 1.8 mM $CaCl_2$, 10 mM glucose, and 25 mM Hepes (pH 7.4). Cells were resuspended at 10^6 cells per ml in this buffer, and 2-ml samples were loaded into a fluorimeter (LS-5B; Perkin-Elmer Cetus Corp., Norwalk, CT) for measurements of intracellular calcium. Excitation and emission wavelengths were 399 and 510 nm, respectively. Maximum calcium–Fura 2 fluorescence was measured after treating loaded cells with 1% Triton X-100 and minimum calcium–Fura 2 fluorescence was measured after the addition of 100 mM Tris, pH 8.0 and 100 mM EGTA.

Results

Purification of rIP-10 Expressed in E. coli. Human and murine IP-10 were generated as recombinant proteins tagged at either the NH_2 or COOH terminus with (His)$_6$. Both NH_2 terminally and COOH terminally His-tagged IP-10 were generated to minimize the possibility that the (His)$_6$ tag could interfere with receptor binding and biological activity or mask a potentially important epitope when raising antibodies to rIP-10. IP-10 was purified by sedimentation of inclusion bodies (which contained the insoluble recombinant protein) through sucrose, solubilization of the inclusion bodies in 4 M guanidine HCl, affinity chromatography on nickel agarose, and then reverse-phase HPLC eluting with an acetonitrile gradient (Fig. 1 *A*). Although there appears to be a shoulder on the IP-10 peak, SDS-PAGE analysis of fractions across this peak revealed a homogenous protein. IP-10 was then radiolabeled with ^{125}I-Bolton and Hunter reagent and subjected to reducing SDS-PAGE (Fig. 1 *B*). Under these purification conditions, IP-10 appears to aggregate into multimers. At the exposure shown in Fig. 1 *B* monomers and dimers are evident; but at longer exposures and on heavily loaded Coomassie-stained gels, higher order multimers are seen. These multimers are reactive with affinity-purified rabbit anti–IP-10 antiserum and are unaffected by reduction and irreversible alkylation of sulfhydryls (data not shown). This aggregation is not the result of the (His)$_6$ tag, since a non-
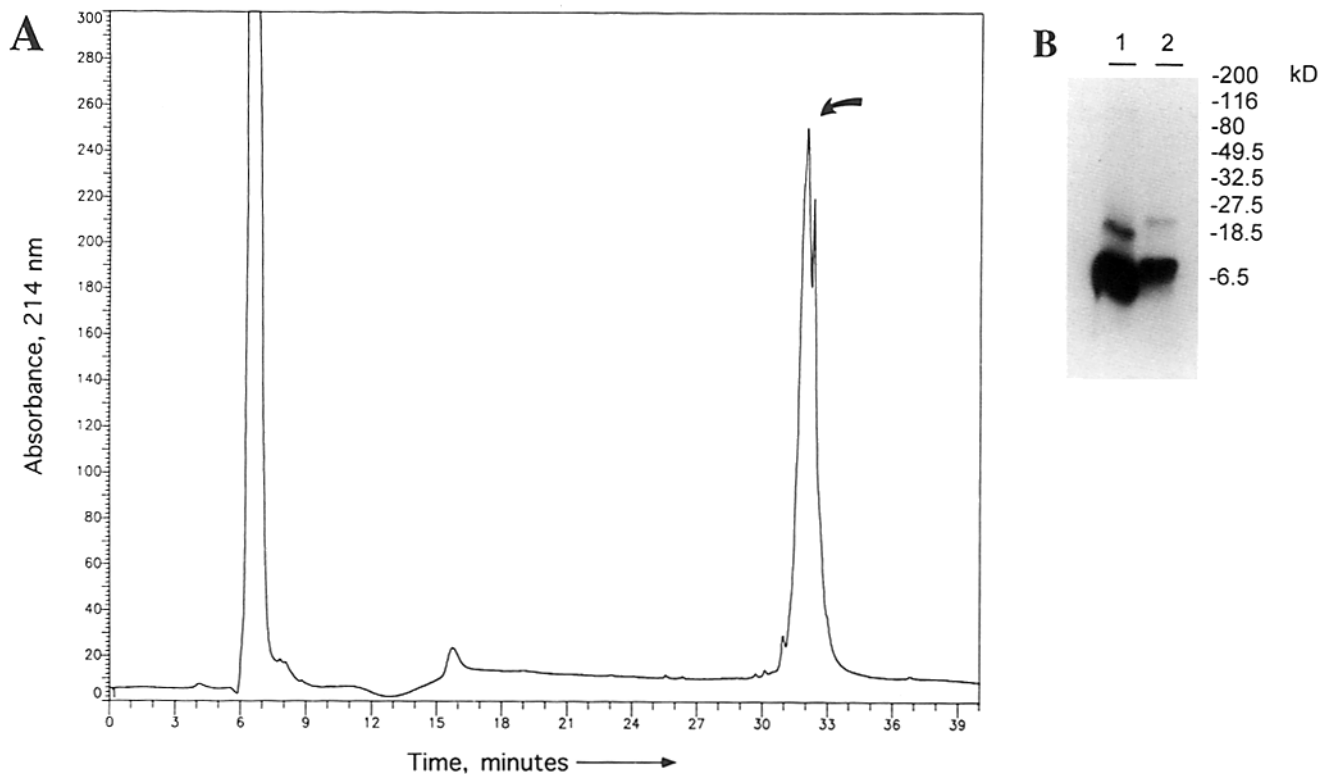
Figure 1. Expression and purification of *E. coli* rIP-10. (*A*) Reverse-phase HPLC purification of rIP-10. Histidine-tagged hIP-10 expressed in *E. coli* was purified on nickel affinity chromatography and the bound fraction was applied to a C-18 Vydac column and eluted with a gradient of acetonitrile. Curved arrow indicates position of IP-10 on A_{214} chromatogram. The first peak that is off scale is the urea-loading buffer. (*B*) 12.5% SDS-PAGE (Tris/Tricine) analysis of Bolton and Hunter ^{125}I-labeled rhIP-10. (Lane *1*) ^{125}I-labeled PeproTech human IP-10 (NEN/Du Pont). (Lane *2*) The (His)$_6$-tagged hIP-10 shown in *A*. The slower migration of the IP-10 monomer and oligomers seen in lane *2* compared with lane *1* is presumably caused by the additional six histidines. Molecular mass markers are indicated to the right of the gel in kilodaltons.

fusion version of IP-10 (Du Pont/NEN) behaved similarily (Fig. 1 *B*).

*Purification of rIP-10 Secreted from J558L Plasmacytoma and CHO Cells.* Since IP-10 purified from *E. coli* aggregated, it was of interest to determine if IP-10 purified from eukaryotic cells and not subjected to denaturation and renaturation would also aggregate. The complete IP-10 cDNA was therefore engineered into the two expression vectors, MoLTR/SV-40 I/pA and pJOD-S, and then stably transfected into J558L and CHO cells, respectively. IP-10 was secreted from both stably transfected lines in similar amounts as judged by a solid-phase ELISA and had similar electrophoretic mobility profiles. IP-10 was purified from conditioned medium by heparin Sepharose affinity chromatography followed by reverse-phase HPLC (Fig. 2). This purification demonstrates that IP-10 binds to heparin Sepharose at physiological NaCl concentrations and is eluted beteween 0.5 M and 1.0 M NaCl (Fig. 2 *A*). The 1-M eluate from the heparin Sepharose column was subjected to reverse-phase HPLC analysis (Fig. 2 *B*). Fractions eluted with a gradient of increasing acetonitrile were analyzed by SDS-PAGE and immunoblotted with an affinity-purified anti–IP-10 antiserum (Fig 2 *C*). The fraction containing immunoreactive IP-10 is indicated on the chromatogram in Fig. 2 *B* by an arrow. IP-10 secreted and purified from eukaryotic cells also aggregates under these purification and elec-

trophoresis conditions (Fig. 2, *A* and *C*). The aggregation of the *E. coli* synthesized material is therefore not unique to the bacterial product and reflects a property of the molecule. Furthermore, the *E. coli*– and J558L-produced IP-10 have the same reverse phase HPLC elution profile (compare position of curved arrow on chromatogram in Fig. 1 *A* with position of curved arrow on chromatogram in Fig. 2 *B*), suggesting they have similar properties.

IP-10–AP Binding to Cells is Specific, Saturable, and Competed by PF4. Since radiolabeled rIP-10 produced in *E. coli* aggregated in solution and on cell surfaces (see below), it was impossible to identify a specific saturable IP-10 binding site. To overcome this problem, IP-10 was expressed as an AP fusion gene that, when introduced into mammalian cells, resulted in the secretion of a nonaggregating monomeric fusion protein that bound to cells via its NH$_2$-terminal IP-10 epitope and enzymatically assayed via its COOH-terminal AP tail (Fig. 3). Both murine (m) and human (h)IP-10 were engineered into the APtag vector and initially used for binding studies. However, since no species specificity was apparent and the murine fusion protein had less nonspecific binding, all data presented in this report used the murine IP-10–AP AP fusion protein (IP-10–AP). The specific activity of the IP-10–AP was estimated by determining the amount of AP activity in 1 ml of conditioned medium and then estimating the amount of
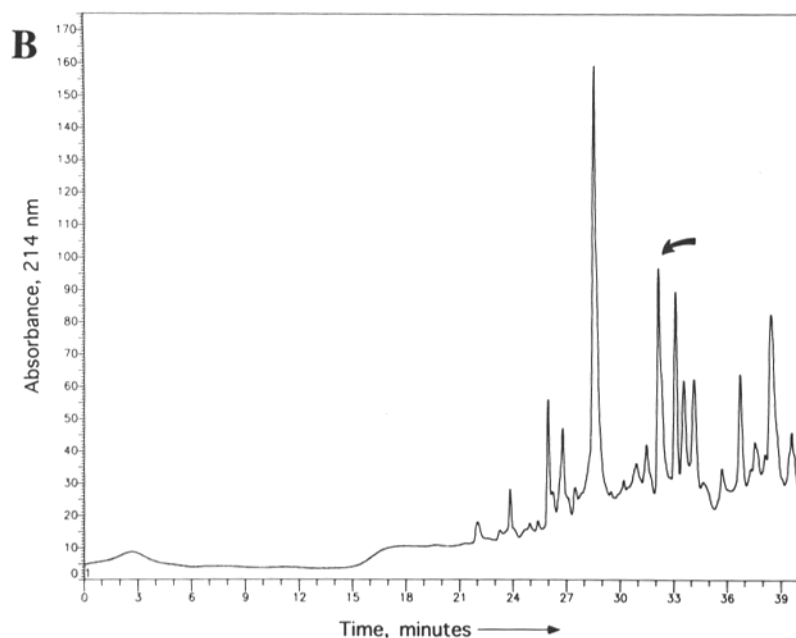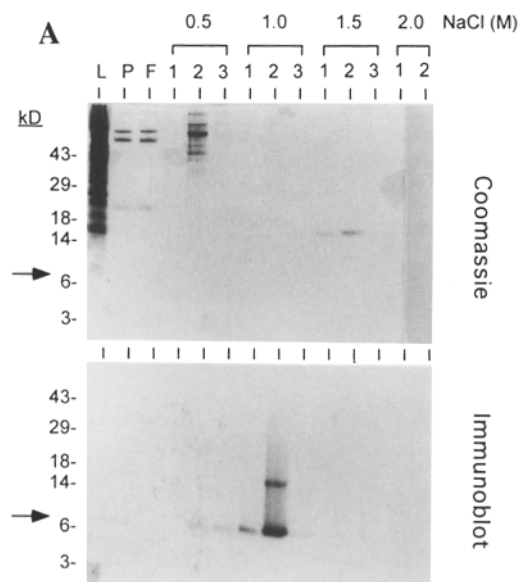
Figure 2. Purification of recombinant IP-10 secreted from J558L cells. Heparin Sepharose affinity chromatography of serum-free conditioned medium collected from J558L cells transfected with a human IP-10 cDNA expression construct analyzed by reverse phase HPLC. (*A, top panel*) Coomassie stained 12.5% SDS-PAGE (Tris/Tricine) of fractions eluted step-wise from a heparin Sepharose column with the indicated concentrations of NaCl. (*A, bottom panel*) Immunoblot of equivalent gel stained with affinity-purified rabbit anti–hIP-10 antibody. *L*, cell lysate; *P*, precolumn; *F*, column flow through. Lanes *1–3* represent sequential fractions collected at the NaCl concentration indicated above the number. (*B*) Reverse-phase HPLC profile of 1 M NaCl eluate from heparin Sepharose column. (*C*) 12.5% SDS-PAGE of HPLC fractions shown in *B*. (*Top panel*) Coomassie-stained gel. (*Bottom panel*) Immunoblot using affinity-purified rabbit anti–IP-10 antiserum. Dotted arrow indicates direction of increasing acetonitrile concentration. Solid arrows indicate position of monomeric IP-10. Molecular mass markers are indicated to the left of the gel in kilodaltons. Curved arrow in *B* indicates IP-10 peak as determined by immunoblot of HPLC fractions shown in *C*.
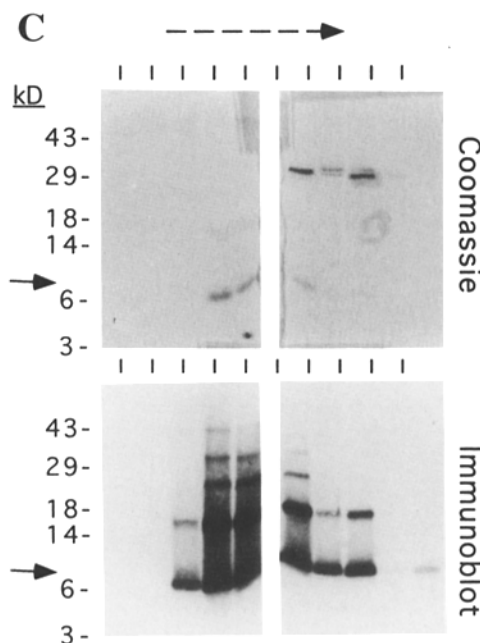
IP-10–AP protein by quantitative immunoprecipitation using an mAb specific for AP.

Using IP-10–AP, we have been able to demonstrate that IP-10 binds specifically to a variety of cells and binds with a K_d of 25 nM on A20 B cells (Fig. 4 *A*). IP-10–AP binding was 100% inhibited by 10 μM recombinant murine or human IP-10 on A20 B cells and EL4 T cells; however, when other chemokines were tested for their ability to compete for IP-10–AP binding to A20 B cells and EL4 T cells, only hPF4 could inhibit 100% of mIP-10–AP binding. At ~100-fold molar excess, hIL-8, hMIP-1α, hMIP-1β, hRANTES had virtually no effect, but hMCP-1 did partially compete (data not shown). Since hMCP-1 partially competed in one experiment, we performed a dose-inhibition experiment comparing

mIP-10, hPF4, and hMCP-1 (Fig. 4 *B*). In this experiment, while hPF4, mIP-10, and heparin (see below) could compete for IP-10–AP binding to cells in a dose-dependent manner, hMCP-1 had no effect on mIP-10–AP, binding even at 100 μg/ml (~10 μM or ~600-fold molar excess). The discrepancy between the two experiments could relate to a change in the source of hMCP-1 (initially from Genentech and then from PeproTech). Of note, the inhibition curve using *E. coli* produced IP-10 was shifted to the right probably because the effective molarity of the IP-10 solution was lower than expected because of the aggregation of rIP-10.

IP-10–AP Inhibits the Aggregation of IP-10 on Cells. To test the hypothesis that the AP tail of the IP-10–AP fusion protein was inhibiting the aggregation of IP-10 on the cell sur-

A

B
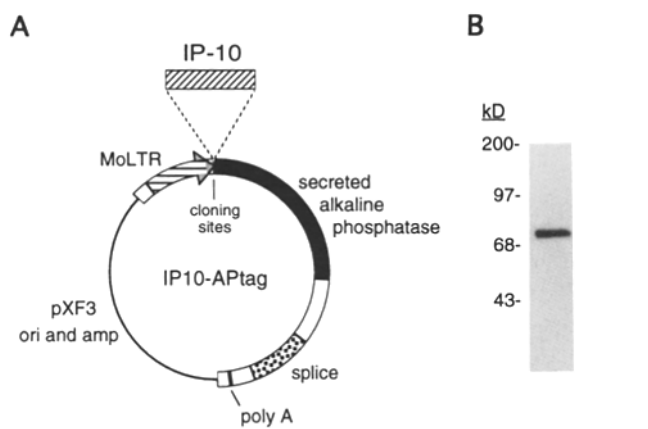
Figure 3. IP-10-AP. (*A*) Schematic of mammalian expression vector APtag. This plasmid carries high level transcription control elements from the Moloney murine leukemia virus LTR, 3' splice, and polyadenylation signals from the rat insulin gene and a domain of the human placental alkaline phosphatase gene. Inserting the murine IP-10 cDNA into the cloning site results in the creation of an IP-10-AP fusion gene. (*B*) Conditioned

face, A20 B cells were incubated with ^{125}I-hIP-10 in the presence of increasing concentrations of either unlabeled hIP-10 or IP-10-AP. As can be seen in Fig. 5, the addition of cold competitor hIP-10 resulted in more ^{125}I-hIP-10 binding to cells, whereas the addition of IP-10-AP was able to compete with ^{125}I-hIP-10 binding to intact cells. Thus, the increased binding of ^{125}I-IP-10 to cells in the presence of increasing cold nonfusion IP-10 is likely a consequence of aggregation of IP-10 on the cell surface.

IP-10 Binding Does Not Induce a Calcium Flux in A20, EL4, and THP-1 Cells. Since most chemokines have been reported to induce a transient calcium flux in cells that have specific cell surface receptors, we tested the ability of IP-10 to flux calcium in A20 B cells and EL4 T cells. Neither the A20

medium from NIH-3T3 cells transfected with above vector was immunoprecipitated using a mAb to AP, subjected to 10% SDS-PAGE, and then immunoblotted with rabbit antimurine IP-10 antibody.

A

B
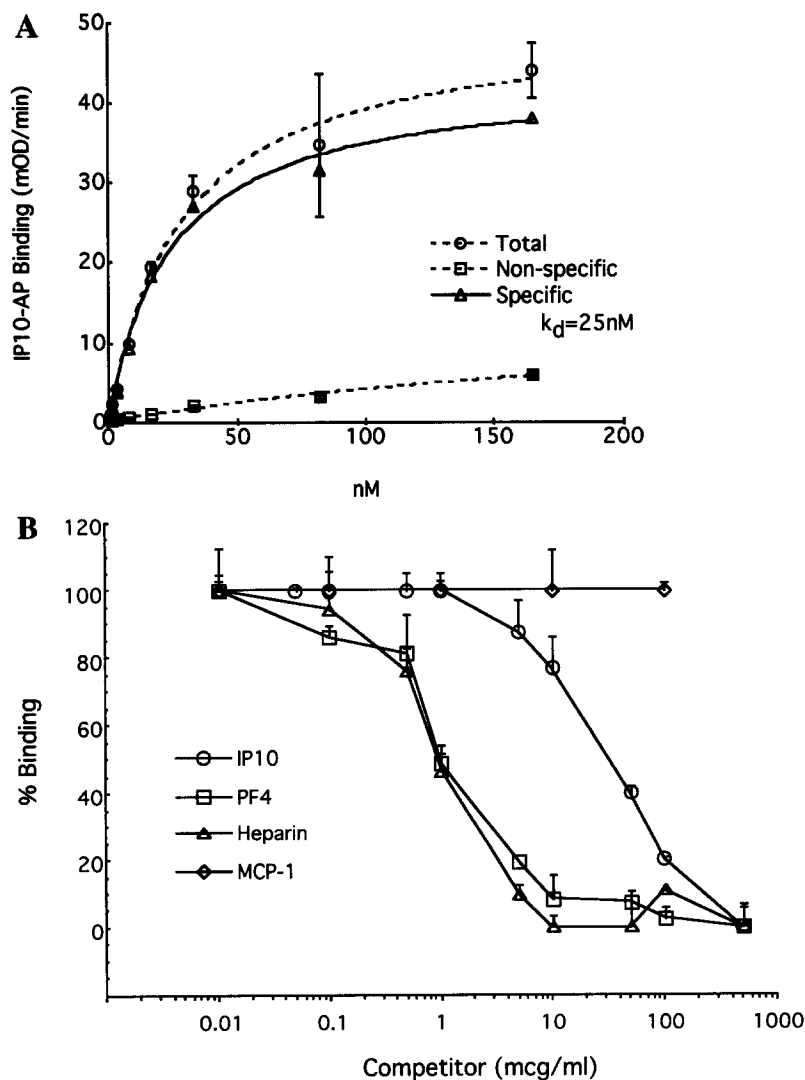
Figure 4. IP-10-AP binding is specific, saturable and competed by PF4 and heparin. (*A*) IP-10-AP binding to A20 B cells. 10^7 A20 B cells were incubated with increasing concentrations of mIP-10-AP. Specific binding = total binding − nonspecific at each point. Nonspecific binding was determined by performing the binding assay at each concentration of IP-10-AP in the presence of excess (10 µM) unlabeled murine rIP-10. (*B*) Concentration-dependent inhibition. 10^7 A20 B cells were incubated with 15 nM murine IP-10-AP in presence of the indicated concentrations of unlabeled recombinant chemokines or heparin for 2 h at 4°C. Cells were then washed and bound IP-10-AP was assayed. Data is presented as the percentage of binding = (binding in presence of competitor minus nonspecific binding/binding in the absence of competitor − nonspecific binding) × 100. Nonspecific binding was determined by the amount of human IL-4-AP or secreted AP bound to murine A20 cells and was usually <1% of the total binding.

225   Luster et al.
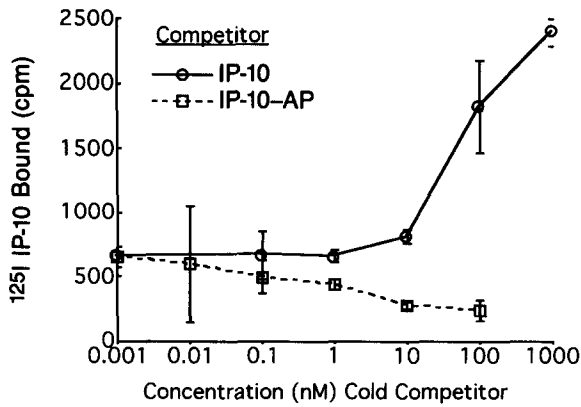
Figure 5. IP-10–AP inhibits aggregation of IP-10 on cell surfaces. 2 × 10⁶ A20 cells were incubated for 2 h at 4°C with 10 nM ¹²⁵I-hIP-10 (NEN/Du Pont) in the presence of the indicated concentrations of unlabeled IP-10 or IP-10–AP fusion protein. The cells were then washed 5× with binding buffer and assayed for cell-bound ¹²⁵I-hIP-10.

or EL4 cell lines fluxed calcium in response to recombinant *E. coli-* or J558L- produced mIP-10 or to mIP-10–AP, even though the A20 B cell line fluxed calcium following crosslinking of its membrane bound IgG with an anti-IgG$_{2b}$ mAb (data not shown). We also tested the responsiveness of the THP-1 cell line to IP-10 stimulation. THP-1 cells are a monocytic cell line that can specifically bind IP-10 (albeit at lower levels than the A20 or EL4 cell lines) and have been reported to flux calcium to various chemokines. The data shown in Fig. 6 *A* demonstrates that the binding of mIP-10–AP to THP-1 cells can be inhibited by excess human or mouse IP-10, but not by hMIP-1α or hMIP-1β. HL60 cells do not bind mIP-10–AP and were included as a negative control. As can be seen in Fig. 6 *B*, THP-1 cells loaded with Fura-2 were able to demonstrate a transient calcium flux upon stimulation with hMCP-1, hRANTES, and hMIP-1α, but were unable to flux calcium upon addition of hIP-10. Furthermore, hIP-10 was unable to desensitize THP-1 cells to subsequent hMCP-1 or hRANTES stimulation. In contrast, hMIP-1α desensitized THP-1 cells to subsequent hRANTES or hMCP-1 stimulation. In addition, heparin and heparan sulfate (100 ng/ml), molecules that augment IL-8 signal transduction (31), did not enable IP-10 to signal (data not shown).

Glycosaminoglycan Inhibition of IP-10 Binding. Heparin and heparan sulfate were able to completely block IP-10–AP binding to cells in a concentration-dependent manner (Fig. 7). Chondroitin sulfate B (dermatan sulfate) was also able to inhibit IP-10–AP binding to A20 B cells, but at higher concentrations than heparin or heparan sulfate. In contrast, chondroitin sulfate A had no effect on IP-10–AP binding, even at 1 mg/ml, whereas heparin and HS completely inhibited IP-10–AP binding at 10 μg/ml. In fact, heparin's inhibition curve was almost superimposable on PF4's inhibition curve (Fig. 4 *B*).

Cellular Distribution of IP-10 Binding Sites. Table 1 summarizes the results of multiple experiments showing the cellular distribution and approximate density of IP-10 binding sites on a number of different cell types. IP-10 binding sites are present in higher numbers on adherent cells like endothelial
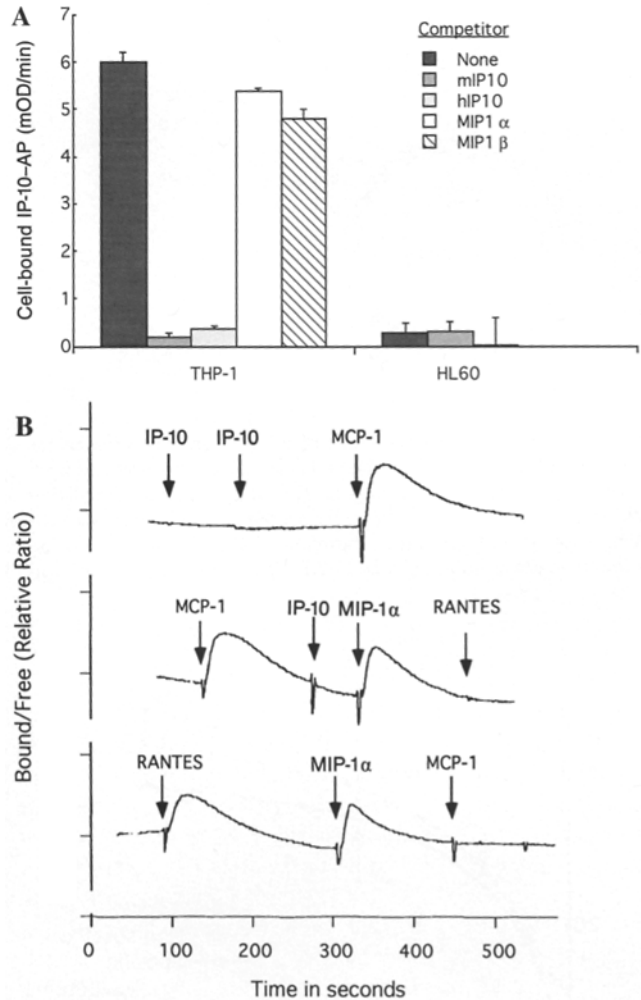
Figure 6. IP-10 binds to the chemokine responsive THP-1 cell line, but does not induce a detectable intracellular calcium flux. (*A*) Specific binding. 10⁷ THP-1 or HL60 cells were incubated for 2 h at 4°C with 15 nM IP-10–AP in the presence of various competitors: none, hIP-10 and mIP10, MIP-1α and MIP-1β (THP-1 cells only). The cells were then washed 5× with HBSS-binding buffer and assayed for cell-bound AP activity. (*B*) Calcium flux. THP-1 cells were loaded with Fura-2 and assayed by spectophotometric methods at 37°C with continuous stirring. Addition of indicated recombinant human chemokine to THP-1 cells is illustrated by arrow. All chemokines were added to a final concentration of 10 nM, except for the second addition of IP-10, which was added to 100 nM.

cells, fibroblasts, and epithelial cells. Furthermore, IFN-γ pretreatment of BM macrophages, U937, THP-1, or HL60 cells did not induce IP-10 binding sites on these cells (data not shown). In addition, the activation of thymocytes with anti-CD3 mAb (2C11) for 24 h had a minimal (approximately twofold) enhancement of IP-10 binding sites. As seen with other cells, however, IP-10 binding to resting or activated thymocytes was inhibited by heparin or HS, and binding was completely lost if the cells were treated with heparinase (data not shown). Unfractionated human peripheral blood leukocytes had trace IP-10 binding that was lost if the cells were passed over nylon wool, indicating that binding sites are located on macrophages or B cells and not on peripheral blood T cells.
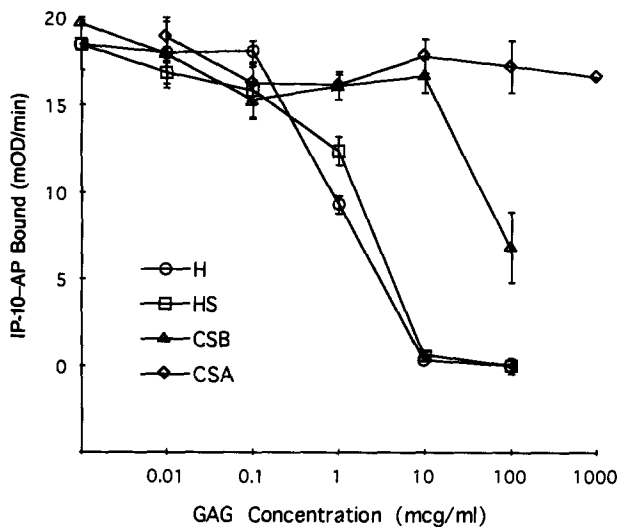
Figure 7. Glycosaminoglycan inhibition of IP-10–AP binding to A20 cells. 10^7 A20 cells were incubated with 15 nM mIP-10–AP in the presence of the indicated concentrations of heparin (H), heparin sulfate (HS), chondroitin sulfate B (CSB), and chondroitin sulfate A (CSA) for 2 h on ice. Cells were then washed and bound IP-10–AP was assayed.

IP-10 Binding to Cells is Dependent on Surface HSPG. Since heparin and heparan sulfate inhibited IP-10–AP binding to cells, and IP-10–AP binding sites were found in higher numbers on adherent cell lines, we tested whether this binding site is salt and heparinase sensitive. Fig. 8 *A* demonstrates that the IP-10–AP binding site on fibroblasts is also competed for by heparin and excess IP-10, and that it is sensitive to heparinase treatment and an 1-M NaCl wash. Heparinase I treatment of BALB/c-3T3 cells enzymatically removed ~75% of the IP-10–AP binding sites while having no effect on kit–AP binding to the kit ligand. Heparinase III also removed ~84%

of the IP-10–AP binding sites on NIH-3T3 cells (data not shown). This is also true for the binding site on A20 B cells, where Heparinase I and III removed 100 and 75%, respectively (data not shown). In addition, after binding and washing in HBSS, a 1-min wash in HBSS adjusted to 1 M NaCl removed all of the IP-10–AP from BALB/c-3T3 and only 50% of kit–AP from these same cells.
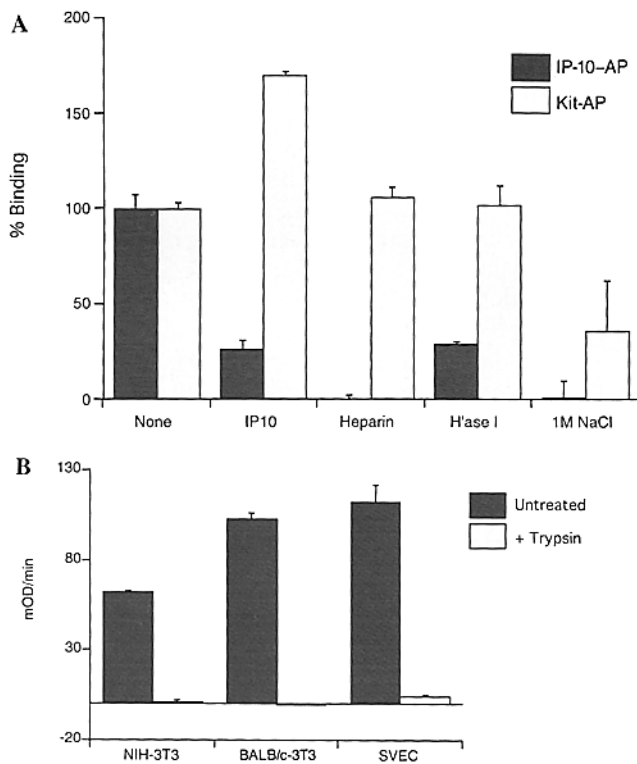
The IP-10 binding site is also sensitive to trypsin digestion on three cell lines tested, NIH-3T3, BALB/c-3T3, and SVEC, a mouse endothelial cell line (Fig. 8 *B*). A further demonstration that IP-10 binding is dependent on cell surface heparan sulfate comes from studies using two CHO mutants that lack HSPG because of mutations in enzymes that are necessary for glycosaminoglycan biosynthesis. As can be seen in Fig. 9, IP-10–AP binds to wild-type parental CHO line K1, but does not bind to either of the mutant lines, 677 and 803. Furthermore, soluble heparan sulfate does not restore binding to the mutants, but in fact, inhibits the binding of IP-10–AP to the wild-type CHO cells in a concentration-dependent fashion.

IP-10 Inhibits HUVEC Proliferation. Since PF4 was able to compete with IP-10 for binding to several cell lines tested, including A20 B cells and NIH 3T3 cells, and since PF4 was known to inhibit bFGF-induced proliferation of endothelial cells, the effect of IP-10 on the growth of HUVECs was tested (Fig. 10 *A*). Like PF4, which has an IC_{50} of 100–200 nM, IP-10 half maximally inhibits HUVEC proliferation at 150 nM (1.5 µg/ml). However, it required at least fivefold more IP-10 to reach 100% inhibition compared to PF4, which again may reflect a propensity of IP-10 to aggregate at high concentrations, decreasing its effective molarity. The inhibition by submaximal concentrations of PF4 and IP-10 are additive (data not shown). As is the case for PF4, increasing concentrations of exogenous heparin reverses the inhibitory effects

Table 1. *Expression of IP-10 Binding Sites by Different Cell Types*

Cell Type	Cell line	Approximate No. of sites/cell	Nondetectable
Endothelial	SVEC	400,000	
Fibroblast	NIH/3T3	330,000	
	Balbc/3T3	165,000	
Epithelial	CHO K1	1,650	CHO 833 and 677
Monocytic	THP-1	1,320	U937, J774, RAW 264.7
B lymphocytic	A20, AJ9	660	MIC, BJAB
T lymphocytic	EL4, LBRM	330	JURKAT, HSB, MBP
Leukocytes	Unfractionated	Trace	Nylon passed
BM culture	Macrophages	825	Mast cells
Thymocytes	Resting	165	

Nondetectable indicates there was no significant binding over background binding. Background binding was determined using either cross-species IL4-AP or secreted AP binding to cells. Number of sites per cell was determined by using the specific activity estimated for IP-10–AP (30 mOD/min per ng).

227   Luster et al.

Figure 8. The IP-10 binding site is heparinase, salt, and trypsin sensitive. (*A*) 10^6 BALB/c-3T3 cells were incubated with either 15 nM mIP-10–AP or an equivalent amount of kit–AP in the presence of no competitor (*None*), 1 μM mIP-10, or 100 μg/ml heparin for 2 h at 4°C. Samples labeled H'ase 1 were treated for 30 min at 37°C with heparinase 1 in serum-free medium and then washed with complete medium before the binding assay. After binding, all cells were washed 5× in HBSS; the samples labeled 1 M NaCl received an additional 1-min wash with HBSS adjusted to 1 M NaCl. The amount of bound AP activity was then enzymatically determined. (*B*) 10^7 cells were trypsinized with 0.25% Trypsin/1 mM EDTA for 5 min at room temperature after which they were incubated with 15 nM mIP-10–AP for 2 h at 4°C, washed 5× with HBSS binding buffer, and assayed for bound AP activity. Binding was determined in parallel on an equivalent number of untrypsinized cells. *SVEC*, an SV-40 transformed murine endothelial cell line.
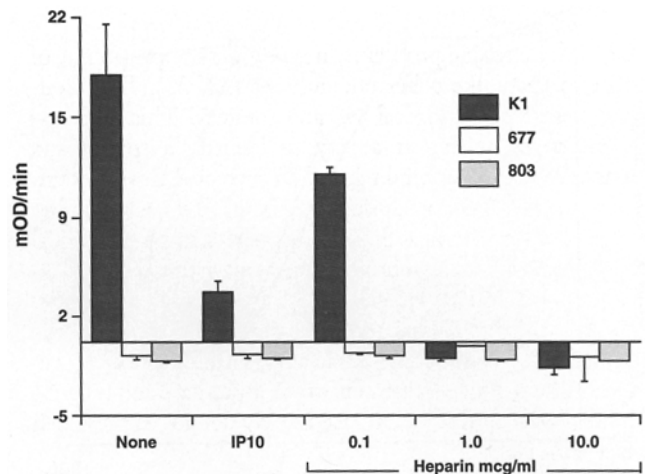
Figure 9. IP-10–AP binds to wild-type CHO (K1) cells but does not bind to the heparan sulfate-deficient mutant CHO cells (677 and 803). 10^6 cells were incubated for 2 h at 4°C with 15 nM IP-10–AP in the presence of 10 μM unlabeled mIP-10 or the indicated concentration of heparin. The monolayers were then washed 5× with HBSS-binding buffer and the amount of bound IP-10–AP was determined.

of IP-10 upon proliferation, just as it does to the inhibitory effects of PF4 (Fig. 10 *B*). A comparison of the binding affinity of each, IP-10 and PF4, for soluble heparin shows the K_d values to be equivalent at 10^{-7} M (Daly, T., personal communication). Neutralizing antibodies to PF4 that block PF4's inhibition of HUVEC proliferation had no effect on IP-10's inhibition of proliferation (data not shown). PF4 and IP-10 do not induce apoptosis in HUVECs; they cause a growth arrest. When PF4 or IP-10 are washed away (by the addition of heparin 5 U/ml) from HUVECs that have been growth arrested by these chemokines and fresh media containing bFGF is added back to the cultures, cellular proliferation resumes (data not shown).
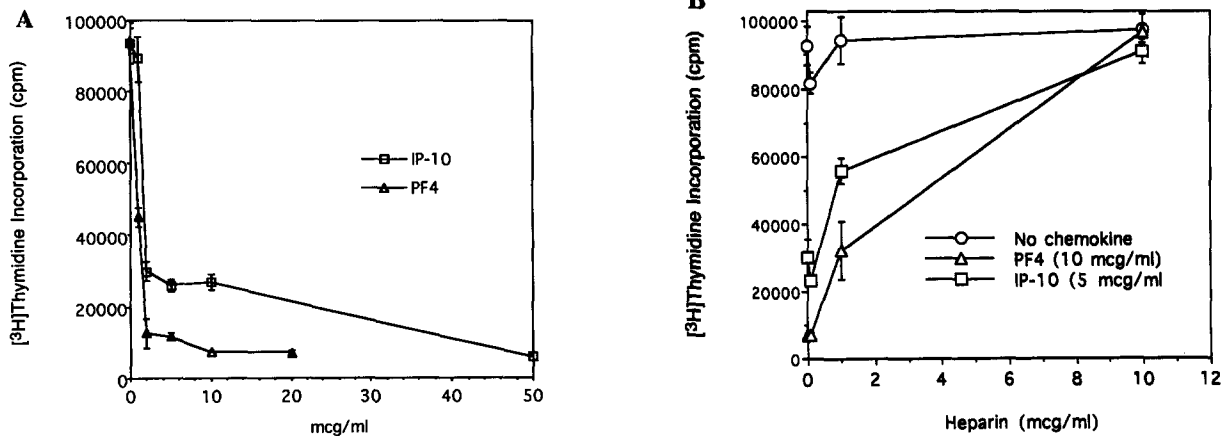
Figure 10. IP-10 inhibits endothelial proliferation, an effect that is antagonized by heparin. (*A*) HUVECs were plated in triplicate in a 96-well plate in the presence of the indicated concentration of hIP-10 or hPF4, 5 ng/ml bFGF, and 10% FBS. The amount of [^{3}H]thymidine incorporated into each well was determined on day 3. (*B*) 6 × 10^3 HUVECs were plated with the bFGF-containing media and with the indicated concentration of heparin alone or with heparin plus 5 μg/ml IP-10 or 10 μg/ml of PF4 for 3 d, and the amount of [^{3}H]thymidine during that period was determined.

Discussion

One of the major problems in studying the properties of IP-10 was that, like other chemokines (32, 33), IP-10 self-aggregates at physiological pH and tonicity. This aggregation interfered with our ability to identify a specific and saturable IP-10 cellular binding site. To overcome this problem, we generated an IP-10–AP fusion protein that retained its ability to bind to cells, but that did not aggregate in physiological buffers. Using this fusion protein, we demonstrated that IP-10 binds to a cell surface HSPG receptor with a K_d of 25 nM. The conclusion that this receptor is a HSPG rests on the observations that cellular IP-10 binding is inhibited by heparin and HS, eliminated by treatment with heparinase and trypsin, and absent on mutant CHO cells that do not express cell surface HSPG.

The binding of IP-10 to its HSPG receptor is a specific interaction. Only PF4 and certain glycosaminoglycans compete for IP-10 binding to cells. Heparin and heparan sulfate are equipotent in competing for IP-10 binding sites, while chondroitin sulfate B is ≥100 fold less potent and chondroitin sulfate A is unable to compete for these sites. Further, PF4 is as potent as heparin in competing with IP-10 binding to cells, while IL-8, RANTES, MIP-1α, MIP-1β, and MCP-1 have virtually no inhibitory effect on IP-10. Although IL-8 binds heparin and is almost as homologous to IP-10 as PF4 (26 vs 31%), it does not effectively compete for IP-10's cellular HSPG sites. Interestingly, human and murine IP-10 competed with murine IP-10–AP and with human IP-10–AP for cellular binding (data not shown), suggesting that there is no binding specificity between these species. It is also striking that IP-10 is less potent on a weight basis than either PF4 or heparin in competing with IP-10–AP binding. This observation is consistent with the formation of IP-10 aggregates, decreasing its effective molar concentration. Aggregation may also explain the fourfold lower K_d found for IP-10 binding to soluble heparin as compared with IP-10–AP binding to cells. Since the monomeric fusion protein IP-10 binds to cells, aggregation of IP-10 is not required for binding to its HSPG receptor. Our approach of using a fusion protein to inhibit self-aggregation might be generally applicable to other chemokines.

We also demonstrated that like PF4, IP-10 inhibits bFGF-induced proliferation of endothelial cells. Moreover, heparin antagonizes this inhibition, suggesting that the antiproliferative effect of IP-10 is mediated through this same HSPG receptor. The specific HSPG site that PF4 and IP-10 share may be a physiologically relevant site at which these molecules modulate the action of other cytokines that use HSPG as part of their receptor complex. For example, PF4 can inhibit both bFGF (15) and TGF-β (16) binding to cells. Indeed, this may be the mechanism whereby PF4 and IP-10 exert their antiproliferative effects and may explain the growth regulating properties that the chemokines have on many diverse cell types (34–37).

Our results do not exclude the possibility that there is another receptor for IP-10. Nonetheless, we were unable to detect an IP-10 binding site on human peripheral lymphocytes,

even though it has been reported that IP-10 is a chemotactic for peripheral blood T cells (10). Furthermore, we have been unable to detect a calcium flux in cells that specifically bind IP-10. It nonetheless remains quite possible that by fusing IP-10 to AP, we have destroyed the ability of IP-10 to interact with its signaling receptor while preserving its ability to interact with a specific HSPG-binding site. Although this is possible, other, albeit nonchemokine alkaline phosphatase fusion proteins (e.g., human and mouse IL-4 [38], kit [27], and fibroblast growth factor receptor (FGFR) [39]) retain their ability to interact with their specific cell-surface receptor or ligands.

One other role for heparin and cell surface HSPG is in enhancing signaling of cytokines to their signaling receptor chains. For example, FGF signaling through its tyrosine kinase receptor, FGFR1, requires either soluble or cell surface–bound HSPG (40). The HSPG receptor betaglycan is also involved in TGF-β signaling. Betaglycan presents TGF-β directly to the serine/threonine kinase subunit of the signaling receptor, forming a high affinity ternary complex (41). It has been demonstrated that heparin and heparan sulfate enhance neutrophil responses to IL-8 (31) and augment the ability of MIP-1β (42) to induce T cell adhesion. The mechanism of this enhancement has not been examined and, indeed, it is not known whether cell surface HSPG or soluble heparin is actually required for chemokines to bind to and signal through their seven transmembrane spanner receptors. This question could be experimentally approached by comparing the ligand binding and signaling properties of wild-type and HSPG-deficient CHO cells that have been transfected with cloned chemokine receptors.

Chemokines are known to bind to heparin, and it has been proposed from studies that found immunoreactive MIP-1β in the distribution of endothelial cells that they bind cell surface HSPG (42). HSPG on cell surfaces may capture chemokines from the fluid phase, thereby immobilizing and establishing a gradient of chemokine that can then be presented to rolling leukocytes and perhaps serve as a substrate for chemotaxis or hapotaxis (43). The specificity of the chemokine–HSPG interaction may play a role in regulating leukocyte homing and the recruitment of leukocytes to sites of inflammation. This could be accomplished through the differential expression of specific HSPG on endothelial cells in different tissues, or through the induction of specific HSPG by specific inflammatory stimuli. The expression of HSPGs with affinity for only a subset of chemokines in a given microenvironment would then allow only those chemokines captured in that microenvironment to be presented to rolling leukocytes. Thus, those chemokines with affinity for the regionally expressed or induced HSPG would be able to more effectively deliver a signal to circulating leukocytes. This hypothesis has not been explored for the chemokines, but the concept of HSPG–ligand specificity dictating a biological response has been established for the FGF family (44).

Constitutive expression of IP-10 is seen in the thymus and in the spleen, and high levels of expression are seen in various

inflammatory conditions. It is therefore useful to consider the possibility that IP-10 plays a role in regulating immune and inflammatory responses by modulating the action of other cytokines that use HSPG as part of their receptor complex. Both IP-10 and PF4 have been demonstrated to inhibit the growth of tumors (9, 45), possibly through immunologic, inflammatory, and/or angiostatic mechanisms. PF4 is in fact now in clinical trials as an antitumor agent. In preliminary experiments, we have shown that injection of IP-10 into a tumor transplant site has an antitumor effect (Luster, A. D., and P. Leder, unpublished observation). In considering the pharmacological delivery of IP-10 or PF4 to tumors, one should bear in mind HSPG receptors may be expressed on the tumor cells themselves, as well as on the endothelial and inflammatory cells that may be a part of the effector mechanism in the antitumor response.

Address correspondence to Andrew D. Luster, Infectious Disease Unit, Massachusetts General Hospital-East, 149 13th St., Charlestown, MA 02129.

References

1. Luster, A.D., J.C. Unkeless, and J.V. Ravetch. 1985. Gamma-interferon transcriptionally regulates an early-response gene containing homology to platelet proteins. *Nature (Lond.)*. 315:672–676.

2. Vanguri, P., and J.M. Farber. 1990. Identification of CRG-2. An interferon-inducible mRNA predicted to encode a murine monokine. *J. Biol. Chem.* 265:15049–15057.

3. Ohmori, Y., and T.A. Hamilton. 1990. A macrophage LPS-inducible early gene encodes the murine homologue of IP-10. *Biochem. Biophys. Res. Commun.* 168:1261–1267.

4. Gottlieb, A.B., A.D. Luster, D.N. Posnett, and D.M. Carter. 1988. Detection of a gamma interferon-induced protein IP-10 in psoriatic plaques. *J. Exp. Med.* 168:941–948.

5. Smoller, B.R., A.D. Luster, J.F. Krane, J. Krueger, M.H. Gray, N.S. McNutt, A. Hsu, and A.B. Gottlieb. 1991. Fixed drug eruptions: evidence for a cytokine-mediated process. *J. Cutaneous Pathol.* 18:13–19.

6. Kaplan, G., A.D. Luster, G. Hancock, and Z.A. Cohn. 1987. The expression of a gamma interferon-induced protein (IP-10) in delayed immune responses in human skin. *J. Exp. Med.* 166:1098–1108.

7. Gomez-Chiarri, M., A. Ortiz, D. Seron, E. Gonzalez, and J. Egido. 1993. The intercrine superfamily and renal disease. *Kidney Int.* 43:S81–S85.

8. Ransohoff, R.M., T.A. Hamilton, M. Tani, M.H. Stoler, H.E. Shick, J.A. Major, M.L. Estes, D.M. Thomas, and V.K. Tuohy. 1993. Astrocyte expression of mRNA encoding cytokines IP-10 and JE/MCP-1 in experimental autoimmune encephalomyelitis. *FASEB (Fed. Am. Soc. Exp. Biol.) J.* 7:592–600.

9. Luster, A.D., and P. Leder. 1993. IP-10, A -C-X-C- chemokine, elicits a potent thymus-dependent antitumor response in vivo. *J. Exp. Med.* 178:1057–1065.

10. Taub, D.D., A.R. Lloyd, K. Conlan, J.M. Wang, J.R. Ortaldo, A. Harada, K. Matsushima, D.J. Kelvin, and J.J. Oppenheim. 1993. Recombinant human interferon-inducible pro-tein 10 is a chemoattractant for human monocytes and T lymphocytes and promotes T cell adhesion to endothelial cells. *J. Exp. Med.* 177:1809–1814.

11. Springer, T.A. 1994. Traffic signals for lymphocyte recirculation and leukocyte emigration: the multistep paradigm. *Cell.* 76:301–314.

12. Murphy, P.M. 1994. The molecular biology of leukocyte chemoattractant receptors. *Annu. Rev. Immunol.* 12:593–633.

13. Busch, C., J. Dawes, D.S. Pepper, and A. Wasteson. 1980. Binding of platelet factor 4 to cultured human umbilical vein endothelail cells. *Biochem. Biophys. Res. Commun.* 19:129–137.

14. Rybak, M.E., M.A.J. Gimbrone, P.F. Davies, and R.I. Handin. 1990. Interaction of platelet factor four with cultured vascular endothelial cells. *Blood.* 73:1534–1539.

15. Sato, Y., M. Abe, and R. Takaki. 1990. Platelet factor 4 blocks the binding of basic fibroblast growth factor to the receptor and inhibits the spontaneous migration of vascular endothelial cells. *Biochem. Biophys. Res. Commun.* 172:595–600.

16. Whitson, R.H., W.L. Wong, and K. Itakura. 1991. Platelet factor 4 selectively inhibits binding of TGF-beta 1 to the type I TGF-beta receptor. *J. Cell. Biochem.* 47:31–42.

17. O'Connell, K.A., and M. Edidin. 1990. A mouse lymphoid endothelial cell line immortalized by simian virus 40 binds lymphocytes and retains functional characteristics of normal endothelial cells. *J. Immunol.* 144:521–525.

18. Esko, J.D. 1992. Animal cell mutants defective in heparan sulfate polymerization. *Adv. Exp. Med. Biol.* 313:97–106.

19. Lidholt, K., J.L. Weinke, C.S. Kiser, F.N. Lugemwa, K.J. Bame, S. Cheifetz, J. Massague, U. Lindahl, and J.D. Esko. 1992. A single mutation affects both N-acetylglucoaminyltransferasae and glucuronosyltransferase activities in a Chinese hamster ovary cell mutant defective in heparan sulfate biosynthesis. *Proc. Natl. Acad. Sci. USA.* 89:2267–2271.

20. Celada, A., P.W. Gray, E. Rinderknecht, and R.D. Schreiber. 1984. Evidence for a gamma-interferon receptor that regulates

macrophage tumoricidal activity. *J. Exp. Med.* 160:55–74.

21. Razin, E., J.N. Ihle, D. Seldin, J. Mencia-Huerta, H.R. Katz, P.A. LeBlanc, A. Hein, J.P. Caulfield, K.F. Austen, and R.L. Stevens. 1984. Interleukin 3: a differentiation and growth factor for the mouse mast cell that contains chondroitin sulfate E proteoglycan. *J. Immunol.* 132:1479–1486.

22. Barsoum, J. 1990. Laboratory Methods: Introduction of stable high-copy-number DNA into Chinese hamster ovary cells by electroporation. *DNA Cell Biol.* 9:293–300.

23. Urlaub, G., and L.A. Chasin. 1980. Isolation of Chinese hamster cell mutants deficient in dihydrofolate reductase activity. *Proc. Natl. Acad. Sci. USA.* 77:4216–4220.

24. Potter, H., L. Weir, and P. Leder. 1984. Enhancer-dependent expression of human kappa immunoglobulin genes introduced into mouse pre-B lymphocytes by electroporation. *Proc. Natl. Acad. Sci. USA.* 81:7161–7165.

25. Luster, A.D., and J.V. Ravetch. 1987. Biochemical character-ization of a gamma interferon-inducible cytokine (IP-10). *J. Exp. Med.* 166:1084–1097.

26. Schagger, H., and G. von Jagon. 1987. Tricine-sodium dodecyl sulfate-polyacrylamide gel electrophoresis for the separation of proteins in the range from 1 to 100 kDa. *Anal. Biochem.* 166:368–379.

27. Flanagan, J.G., and P. Leder. 1990. The kit ligand: a cell sur-face molecule altered in steel mutant fibroblasts. *Cell.* 63:185–194.

28. Limbird, L.E. 1986. Cell Surface Receptors: A Short Course on Theory and Methods. Martinus Nijhoff Publishers, Boston, MA. pp. 51–96.

29. Bashkin, P., S. Doctrow, M. Klagsburn, S. Magnus, J. Folkman, and I. Vlodavsky. 1989. Basic fibroblast growth factor binds to subendothelial extracellular matrix and is released by heparitinase and heparin-like molecules. *Biochemistry.* 28:1737–1743.

30. Maione, T.E., G.S. Gray, J. Petro, A.J. Hunt, A.L. Donner, S.I. Bauer, H.F. Carson, and R.J. Sharpe. 1990. Inhibition of angiogenesis by recombinant human platelet factor-4 and related peptides. *Science (Wash. DC).* 247:77–79.

31. Webb, L.M., M.U. Ehrengruber, L.I. Clark, M. Baggiolini, and A. Rot. 1993. Binding to heparan sulfate or heparin en-hances neutrophil responses to interleukin 8. *Proc. Natl. Acad. Sci. USA.* 90:7158–7162.

32. Lodi, P.J., D.S. Garrett, J. Kuszewski, M.L. Tsang, J.A. Weatherbee, W.J. Leonard, A.M. Gronenborn, and G.M. Clore. 1994. High-resolution solution structure of the beta chemokine hMIP-1 beta by multidimensional NMR. *Science (Wash. DC).* 263:1762–1767.

33. Mantel, C., Y.J. Kim, S. Cooper, B. Kwon, and H.E. Brox-meyer. 1993. Polymerization of murine macrophage inflam-matory protein 1a inactivates its myelosuppressive effects in vitro: The active form is a monomer. *Proc. Natl. Acad. Sci. USA.* 90:2232–2236.

34. Han, Z.C., L. Sensebe, J.F. Abgrall, and J. Briere. 1990. Platelet factor 4 inhibits human megakaryocytopoiesis in vitro. *Blood.* 75:1234–1239.

35. Gregg, E.O., L. Yarwood, M.J. Wagstaffe, D.S. Pepper, and M.C. MacDonald. 1990. Immunomodulatory properties of platelet factor 4: prevention of concanavalin A (Con A) suppres-sor-induction in vitro and augmentation of an antigen-specific delayed-type hypersensitivity response in vivo. *Immunology.* 70:230–234.

36. Han, Z.C., A.M. Maurer, S. Bellucci, H.Y. Wan, Y. Kroviarski, O. Bertrand, and J.P. Caen. 1992. Inhibitory effect of platelet factor 4 (PF4) on the growth of human erythroleukemia cells: proposed mechanism of action of PF4. *J. Lab. Clin. Med.* 120:645–660.

37. Sarris, A.H., H.E. Broxmeyer, U. Wirthmueller, N. Karasavvas, S. Cooper, L. Lu, J. Krueger, and J.V. Ravetch. 1993. Human interferon-inducible protein 10: expression and purification of recombinant protein demonstrates inhibition of early human hematopoietic progenitors. *J. Exp. Med.* 178:1127–1132.

38. Morrison, B.W., and P. Leder. 1992. A receptor binding do-main of mouse interleukin-4 defined by a solid-phase binding assay and in vitro mutagenesis. *J. Biol. Chem.* 267:11957–11963.

39. Ornitz, D.M., A. Yayon, J.G. Flanagan, C.M. Svahn, E. Levi, and P. Leder. 1992. Heparin is required for cell-free binding of basic fibroblast growth factor to a soluble receptor and for mitogenesis in whole cells. *Mol. Cell. Biol.* 12:240–247.

40. Yayon, A., M. Klagsbrun, J.D. Esko, P. Leder, and D.M. Or-nitz. 1991. Cell surface, heparin-like molecules are required for binding of basic fibroblast growth factor to its high affinity receptor. *Cell.* 64:841–848.

41. Lopez-Casillas, F., J.L. Wrana, and J. Massague. 1993. Be-taglycan presents ligand to the TGFb signaling receptor. *Cell.* 73:1435–1444.

42. Tanaka, Y., D.H. Adams, S. Hubscher, H. Hirano, U. Sieben-list, and S. Shaw. 1993. T-cell adhesion induced by proteoglycan-immobilized cytokine MIP-1β. *Nature (Lond.).* 361:79–82.

43. Rot, A. 1992. Endothelial cell binding of NAP-1/IL-8: role in neutrophil emigration. *Immunol. Today* 13:291–294.

44. Nurcombe, V., M.D. Ford, J.A. Wildschut, and P.F. Bartlett. 1993. Developmental regulation of neural response to FGF-1 and FGF-2 by heparan sulfate proteoglycan. *Science (Wash. DC).* 260:103–106.

45. Sharpe, R.J., H.R. Byers, C.F. Scott, S.I. Bauer, and T.E. Maione. 1990. Growth inhibition of murine melanoma and human colon carcinoma by recombinant human platelet factor 4. *J. Natl. Cancer Inst.* 82:848–853.